Journal of Solid State Chemistry 183 (2010) 2253–2260

Contents lists available at ScienceDirect

Journal of Solid State Chemistry

journal homepage: www.elsevier.com/locate/jssc

The first quaternary lanthanide(III) nitride iodides: $NaM_4N_2I_7$ (M=La–Nd)

Christian M. Schurz, Thomas Schleid *

Institut für Anorganische Chemie, Universität Stuttgart, Pfaffenwaldring 55, D-70569 Stuttgart, Germany

ARTICLE INFO

Article history:
Received 12 May 2010
Received in revised form
14 July 2010
Accepted 16 July 2010
Available online 1 September 2010

Keywords:
Trans-edge linked $[NM_4]^{9+}$ tetrahedra
Isolated $[NaI_6]^{5-}$ octahedra
Crystal structures
IR spectra

ABSTRACT

In attempts to synthesize lanthanide(III) nitride iodides with the formula M_2NI_3 (M=La–Nd), moisture-sensitive single crystals of the first quaternary sodium lanthanide(III) nitride iodides $NaM_4N_2I_7$ (orthorhombic, $Pna2_1$; Z=4; a=1391–1401, b=1086–1094, c=1186–1211 pm) could be obtained. The dominating structural features are $^1_\infty\{[NM^e_{4/2}]^{3+}\}$ chains of *trans*-edge linked $[NM_4]^{9+}$ tetrahedra, which run parallel to the polar 2_1-axis [001]. Between the chains, direct bonding via special iodide anions generates cages, in which isolated $[NaI_6]^{5-}$ octahedra are embedded. The IR spectrum of $NaLa_4N_2I_7$ recorded from 100 to 1000 cm^{-1} shows main bands at υ=337, 373 and 489 cm^{-1}. With decreasing radii of the lanthanide trications these bands, which can be assigned as an influence of the vibrations of the condensed $[NM_4]^{9+}$ tetrahedra, are shifted toward higher frequencies for the $NaM_4N_2I_7$ series (M=La–Nd), following the lanthanide contraction.

1. Introduction

Up to now only five single-crystal structure investigations of quaternary nitride halides, namely K_2OsNCl_5 [1], $Ba_4WN_4Cl_2$ [2], $Ba_{25}Nb_5N_{19}Cl_{18}$, $Ba_3Ta_3N_6Cl$ and $Ba_{15}Ta_{15}N_{33}Cl_4$ [3–5], have been reported in literature. Other compounds often form just non-stoichiometric intercalates of the correlative ternary nitride halides, e.g. Li_xZrNCl [6] and Na_xHfNCl [7,8]. On the other hand, new developments could be obtained in the chemistry of lanthanide nitride halides known with the formulae M_2NCl_3 (M=La–Nd, Gd) [9–11], M_2NBr_3 (M=Ce, Gd) [12], M_3NCl_6 (M=Ce, Nd, Gd) [13–15], M_3NBr_6 (M=La, Ce) [12,16] and the only well-characterized lanthanide nitride iodide $Ce_{15}N_7I_{24}$ [17] recently. Apart from these, a quinary compound of the composition $Cs_{1-x}Na_xLa_9N_4I_{16}$ [18] has been described with an unusual mixed and underoccupied Cs^+/Na^+ position. In all these nitride halides, nitride-centered lanthanide tetrahedra $[NM_4]^{9+}$ can be found, but there are different ways, in which these tetrahedra participate in the different crystal structures. For the nitride-poor compounds M_3NCl_6 (M = Ce, Nd, Gd) and M_3NBr_6 (M = La, Ce) isolated bitetrahedra $[N_2M_6]^{12+}$ as pairs of two edge-connected $[NM_4]^{9+}$ units prevail, according to the doubled formula $M_6N_2X_{12}$ (X=Cl and Br), while in the M_2NCl_3 (M = La–Nd, Gd) and M_2NBr_3 representatives (M=Ce, Gd) the dominating structural features are infinite $^1_\infty\{[NM^e_{4/2}]^{3+}\}$ chains of *trans*-edge shared $[NM_4]^{9+}$ tetrahedra as well as for $Cs_{1-x}Na_xLa_9N_4I_{16}$. Completely isolated $[NM_4]^{9+}$ tetrahedra occur for example in quaternary lanthanide(III) nitride sulfide chlorides with the formula $M_4NS_3Cl_3$ (M=La–Nd) [15,19], whereas in the crystal structure of $Ce_{15}N_7I_{24}$, again $^1_\infty\{[NM^e_{4/2}]^{3+}\}$ chains, but surprisingly also threefold bonded nitride anions in $[NM_3]^{6+}$ triangles are present simultaneously. Since no M_3NI_6- and M_2NI_3-type nitride iodides were known so far, attempts for their syntheses seemed necessary. Obtained instead, a structural description of the first quaternary nitride iodides with sodium with the composition $NaM_4N_2I_7$ (M=La–Nd) [20] is presented in this study, as well as the first infrared spectra of nitride- and halide-containing quaternary lanthanide compounds.

2. Experimental

2.1. Syntheses

Single crystals of all four members of the short $NaM_4N_2I_7$ series (M=La–Nd) were synthesized by using the respective lanthanide metal (M: ChemPur, 99.9%), the corresponding triiodides (MI_3: Sigma Aldrich, 99.9+%) and dried sodium azide (NaN_3: E. Merck: 99.9%) in a molar ratio of 8:10:3 while attempting to obtain the M_2NI_3-type nitride iodides. Sodium iodide (NaI: E. Merck, *Suprapur*, 99.9%) was added in excess initially, scheduled just as fluxing agent, but according to the equation

$$16\ M + 20\ MI_3 + 6\ NaN_3 + 3\ NaI \rightarrow 9\ NaM_4N_2I_7$$

it obviously also worked partly as a reactant. All mixtures were loaded into fused silica ampoules, evacuated and sealed,

* Corresponding author. Fax: +49 711 685 64241.
E-mail address: schleid@iac.uni-stuttgart.de (Th. Schleid).

0022-4596/$ - see front matter © 2010 Elsevier Inc. All rights reserved.
doi:10.1016/j.jssc.2010.07.025

afterwards heated at 700 °C for 7 days and cooled to room temperature within 24 h. The reactions lead to air- and moisture-sensitive, transparent, *pseudo*-acicular single crystals in most cases with the color of the respective lanthanide trication (La^{3+}: colorless; Pr^{3+}: yellowish green; Nd^{3+}: pinkish blue). Only $NaCe_4N_2I_7$ with presumably colorless Ce^{3+} cations occurred as a red product.

2.2. Crystal structure analyses

To protect the crystals against contamination by moist air all ampoules were opened in a glove box under argon atmosphere. For low-temperature single-crystal X-ray measurements (100 K) adequate crystals were selected and mounted under the special oil Fomblin®Y (Alfa Aesar) on a κ-CCD single-crystal diffractometer (Bruker–Nonius). This procedure was necessary to prevent the highly moisture-sensitive single crystals from decomposing. The corresponding data sets were calculated with the help of the program package SHELX-97 [21] and investigated more closely with the programs PLATON [22] and MAPLE [23]. Details of the data collections and structure refinements are noted in Table 1. Atomic positions and coefficients of the equivalent isotropic thermal displacement parameters show up in Table 2. Important interatomic distances and motifs of mutual adjunction [23] are given in Tables 3 and 4. The quality of the data sets of the highly moisture sensitive single crystals depends upon the level of their partial decomposition (yellowish discolored frames around single-crystal cores could be observed after the X-ray measurements) and is also due to the *non*-centrosymmetric space group, which turns systematically the crystals into merohedral inversion twins. Further details of the crystal structure investigations can be requested from the Fachinformationszentrum (FIZ) Karlsruhe, D-76344 Eggenstein-Leopoldshafen, Germany (fax: +49(0)7247/808 666; e-mail: crysdata@fiz-karlsruhe.de), on quoting the depository numbers CSD-419946 for $NaLa_4N_2I_7$, CSD-419947 for $NaCe_4N_2I_7$, CSD-419948 for $NaPr_4N_2I_7$, and CSD-419949 for $NaNd_4N_2I_7$.

2.3. Infrared spectroscopy

All IR spectra were recorded on a Fourier-transform IR-spectrometer IFS 113v Bruker Optik (with vacuum optic and Genzel interferometer) with a resolution of $\pm 2\,cm^{-1}$ and analyzed with the program OPUS-NT (OPUS, Version 3.1). To prepare the samples for adequate IR measurements, 1 mg of the dedicated *pseudo*-acicular crystals of the $NaM_4N_2I_7$ representatives with M=La–Nd were taken into a glove box under inert gas atmosphere (either argon or nitrogen) and pressed to pellets with 200 mg potassium bromide (KBr) for the data collections between 400 and 1000 cm^{-1}. For additional information between 100 and 400 cm^{-1}, the samples were pressed to pellets with 150 mg polyethylene (PE), which came out slightly uneven. As a result, reflection effects in all spectra recorded between 100 and 400 cm^{-1} could be detected. Furthermore, the binary substances NaI and MI_3 (M=La–Nd) were measured for comparison and a proper classification of the infrared bands (Table 5).

3. Results and discussion

3.1. Structure description

The first quaternary nitride iodides of the trivalent lanthanides with the composition $NaM_4N_2I_7$ (M=La–Nd) crystallize in the orthorhombic crystal system in the space group $Pna2_1$ (a=1391.35(9)–1400.18(9) pm, b=1082.43(7)–1093.15(7) pm, c=1186.14(8)–1210.21(8) pm) with four formula units per unit cell. Their crystal structure contains four crystallographically different rare-earth metal trications (M^{3+}), two different nitride anions (N^{3-}), seven crystallographically independent iodide anions (I^-) and one sodium cation (Na^+), all at the general *Wyckoff* position 4*a*. With basically trigonal prismatic ($M1$: tricapped, CN=7+*2*; $M4$: bicapped, CN=8; Fig. 1, *left top* and *left mid*) and octahedral ($M2$: bicapped, CN=6+*2*; $M3$: monocapped, CN=6+*1*; Fig. 1, *right top* and *right mid*)

Table 1
Crystallographic data for the quaternary lanthanide nitride iodides $NaM_4N_2I_7$ (M=La–Nd) and their determination.

$NaM_4N_2I_7$	M=La	M=Ce	M=Pr	M=Nd
Crystal system, space group	Orthorhombic, $Pna2_1$ (no. 33)			
Formula units	4			
Lattice parameters				
a (pm)	1400.18(9)	1397.03(9)	1394.12(9)	1391.35(9)
b (pm)	1093.15(7)	1089.32(7)	1085.78(7)	1082.43(7)
c (pm)	1210.21(8)	1201.94(8)	1193.89(8)	1186.14(8)
Calculated density, D_x (g cm^{-3})	5.361	5.446	5.524	5.638
Molar volume, V_m (cm^3 mol^{-1})	278.92	275.42	272.12	269.98
F(000)	2496	2512	2528	2544
Diffractometer, wavelength	Kappa-CCD, Mo-$K\alpha$: λ=71.07 pm			
Index range				
$\pm h$	18	18	18	18
$\pm k$	14	14	14	14
$\pm l$	16	15	15	15
θ range, min/max	0.41/28.28			
Absorption coefficient (μ/mm^{-1})	20.70	21.58	22.55	23.53
Data corrections	Background, polarization, and Lorentz factors; numerical absorption correction: program *HABITUS* [24]			
Collected, unique reflections	23416, 4241	22327, 4359	27443, 3966	20605, 4334
R_{int}, R_σ	0.157, 0.079	0.181, 0.092	0.207, 0.094	0.174, 0.087
Structure solution and refinement	Program package *SHELX-97* [21]			
Scattering factors	International Tables, Vol. C [25]			
R_1, reflections with $\lvert F_o\rvert \geq 4\sigma(F_o)$	0.053, 3971	0.092, 3404	0.063, 3433	0.078, 3085
R_1, wR_2 for all reflections	0.056, 0.125	0.120, 0.198	0.076, 0.142	0.116, 0.156
Goodness of fit (GooF)	1.042	1.064	1.029	1.025
Residual electron density, max	2.41	3.45	2.60	3.28
(ρ/$e^- \cdot 10^{-6}$ pm^{-3}) min	−2.97	−3.39	−2.37	−3.19

Table 2
Atomic coordinates and equivalent isotropic thermal displacement parameters U_{eq}[a] for the quaternary nitride iodides $NaM_4N_2I_7$ (M=La–Nd).

Atom	Wyckoff position	x/a	y/b	z/c	U_{eq}/pm^2	M
Na[b]	4*a*	0.4104(6)	0.4521(8)	1/4	194(19)	La
		0.4072(12)	0.4555(16)	1/4	225(38)	Ce
		0.4061(8)	0.4545(12)	1/4	194(27)	Pr
		0.4059(12)	0.4588(16)	1/4	307(43)	Nd
*M*1	4*a*	0.08896(7)	0.37540(9)	0.31048(11)	51(2)	La
		0.0886(1)	0.3745(2)	0.3118(2)	129(4)	Ce
		0.08738(9)	0.37436(12)	0.31469(14)	69(3)	Pr
		0.0870(1)	0.3750(2)	0.3183(2)	97(4)	Nd
*M*2	4*a*	0.40918(7)	0.11280(9)	0.05248(11)	54(2)	La
		0.4096(1)	0.1110(2)	0.0540(2)	136(4)	Ce
		0.41053(9)	0.10938(13)	0.05664(13)	73(3)	Pr
		0.4107(1)	0.1069(2)	0.0616(2)	92(4)	Nd
*M*3	4*a*	0.39415(7)	0.90721(9)	0.31704(11)	53(2)	La
		0.3952(1)	0.9088(2)	0.3188(2)	134(4)	Ce
		0.39540(9)	0.91097(12)	0.32142(14)	70(3)	Pr
		0.3967(1)	0.9117(2)	0.3257(2)	95(4)	Nd
*M*4	4*a*	0.08743(7)	0.62730(9)	0.07514(11)	51(2)	La
		0.0872(1)	0.6274(2)	0.0766(2)	128(4)	Ce
		0.08618(9)	0.62669(13)	0.08006(12)	71(3)	Pr
		0.0854(1)	0.6275(2)	0.0843(2)	91(4)	Nd
N1	4*a*	0.4951(11)	0.0026(14)	0.1873(16)	87(28)	La
		0.4948(27)	−0.0073(41)	0.1904(38)	235(74)	Ce
		0.4946(14)	0.0043(19)	0.1881(22)	101(40)	Pr
		0.4938(21)	0.0056(33)	0.1939(33)	228(70)	Nd
N2	4*a*	0.4982(11)	0.0124(13)	0.4401(16)	96(28)	La
		0.4983(27)	0.0071(32)	0.4483(36)	202(70)	Ce
		0.5008(15)	0.0153(19)	0.4434(23)	113(43)	Pr
		0.4936(23)	0.0153(31)	0.4516(34)	236(72)	Nd
I1	4*a*	0.03352(9)	0.81815(10)	0.28899(11)	99(2)	La
		0.0317(2)	0.8165(3)	0.2895(2)	171(5)	Ce
		0.0301(1)	0.8154(2)	0.2920(2)	106(3)	Pr
		0.0284(2)	0.8151(3)	0.2941(2)	133(5)	Nd
I2	4*a*	0.24136(9)	0.60355(10)	0.32640(11)	82(2)	La
		0.2398(2)	0.6021(3)	0.3292(2)	161(5)	Ce
		0.2377(1)	0.6000(2)	0.3327(2)	91(3)	Pr
		0.2368(2)	0.5987(3)	0.3384(2)	113(5)	Nd
I3	4*a*	0.01977(9)	0.14434(10)	0.45790(11)	94(2)	La
		0.0184(2)	0.1452(3)	0.4579(2)	169(5)	Ce
		0.0174(1)	0.1452(2)	0.4604(2)	107(3)	Pr
		0.0161(2)	0.1461(3)	0.4624(2)	131(5)	Nd
I4	4*a*	0.05607(9)	0.17236(10)	0.10749(11)	89(2)	La
		0.0551(2)	0.1744(3)	0.1078(2)	172(5)	Ce
		0.0552(1)	0.1761(2)	0.1095(2)	107(3)	Pr
		0.0532(2)	0.1780(3)	0.1122(2)	124(5)	Nd
I5	4*a*	0.25550(9)	0.42063(10)	0.03769(11)	90(2)	La
		0.2548(2)	0.4225(3)	0.0365(2)	161(5)	Ce
		0.2542(1)	0.4256(2)	0.0368(2)	102(3)	Pr
		0.2533(2)	0.4286(3)	0.0394(2)	130(5)	Nd
I6	4*a*	0.29634(9)	0.18744(10)	0.29908(11)	77(2)	La
		0.2952(2)	0.1874(3)	0.2982(2)	146(5)	Ce
		0.2949(1)	0.1881(2)	0.2985(2)	89(3)	Pr
		0.2941(2)	0.1872(3)	0.3001(2)	122(5)	Nd
I7	4*a*	0.26957(9)	0.86837(10)	0.08124(11)	101(2)	La
		0.2704(2)	0.8669(3)	0.0850(2)	177(5)	Ce
		0.2713(1)	0.8658(2)	0.0889(2)	110(3)	Pr
		0.2721(2)	0.8638(3)	0.0954(2)	140(5)	Nd

[a] $U_{eq}=1/3(U_{11}+U_{22}+U_{33})$ [27].
[b] z/c arbitrarily fixed at 1/4 for a proper definition of the origin.

surroundings mainly two different anionic coordination spheres are observed for the M^{3+} cations [26]. Between the shortest and the longest distances the metal-iodide bond lengths are very variable. This is also reflected by the coordination spheres of the

Table 3
Selected interatomic distances (d/pm) and the average distance ($Ø$/pm) of the regular M^{3+}–I^- bonds in the quaternary nitride iodides $NaM_4N_2I_7$ (M=La–Nd).

	M=La d/*pm*	M=Ce d/*pm*	M=Pr d/*pm*	M=Nd d/*pm*
N1–*M*1	239.3	244.3	238.6	234.7
N1–*M*2	235.8	240.7	226.6	223.7
N1–*M*3	235.6	226.5	234.0	230.6
N1–*M*4	235.2	228.5	230.6	232.4
N1–N2	299.8	291.2	292.9	288.4
N1–N2′	306.1	310.5	305.3	306.2
N2–*M*1	236.3	243.9	229.3	236.7
N2–*M*2	232.5	221.9	227.8	227.8
N2–*M*3	237.9	237.6	235.9	230.8
N2–*M*4	238.5	235.0	236.5	227.3
Na–I1	308.3	307.8	308.0	302.8
Na–I2	303.3	299.2	299.7	301.1
Na–I3	312.9	313.6	314.3	315.3
Na–I4	299.8	302.8	302.4	298.8
Na–I5	338.0	335.3	332.6	329.5
Na–I6	335.7	335.4	333.3	337.9
*M*1–I2	328.8	326.4	323.2	320.4
*M*1–I3	324.1	320.7	318.8	316.7
*M*1–I4	334.3	331.5	329.2	327.8
*M*1–I6	356.0	353.7	353.5	353.4
*M*1–I7	383.0	383.1	382.2	382.9
*M*1–I5	407.2	407.6	409.0	407.9
*M*1–I6′	415.7	415.7	413.9	413.5
*M*2–I2	345.5	341.6	338.1	335.0
*M*2–I4	319.2	316.4	314.6	311.7
*M*2–I6	347.4	344.4	341.6	337.5
*M*2–I7	332.9	331.6	330.4	328.6
*M*2–I1	398.1	397.3	395.9	398.3
*M*2–I5	399.8	402.9	407.4	412.2
*M*3–I1	316.1	312.8	311.3	308.7
*M*3–I5	339.7	335.6	331.5	328.8
*M*3–I6	336.3	335.0	333.0	332.0
*M*3–I7	337.1	333.8	330.8	327.6
*M*3–I2	395.1	398.7	403.1	405.6
*M*4–I1	340.9	337.5	334.8	330.8
*M*4–I2	373.6	372.1	369.4	369.0
*M*4–I3	324.0	321.7	320.4	317.6
*M*4–I5	329.4	327.1	324.3	322.1
*M*4–I6	377.4	378.5	380.7	382.0
*M*4–I7	366.8	365.7	366.1	364.8
Ø(M–I)	*342.8*	*340.5*	*338.6*	*336.7*

Table 4
Motifs of mutual adjunction (*italic*≡secondary contacts) in the crystal structure of the quaternary nitride iodide $NaM_4N_2I_7$ (M=La–Nd).

	N1	N2	I1	I2	I3	I4	I5	I6	I7	CN
Na	0/0	0/0	1/1	1/1	1/1	1/1	1/1	1/1	0/0	6
M1	1/1	1/1	0/0	1/1	1/1	1/1	*1/1*	1+*1*/1+*1*	1/1	7+*2*
M2	1/1	1/1	*1/1*	1/1	0/0	1/1	*1/1*	1/1	1/1	6+*2*
M3	1/1	1/1	1/1	*1/1*	0/0	0/0	1/1	1/1	1/1	6+*1*
M4	1/1	1/1	1/1	1/1	1/1	0/0	1/1	1/1	1/1	8
CN	4	4	3+*1*	4+*1*	3	3	3+*2*	5+*1*	4	

iodide anions (see Fig. 2 and Table 4). The shortest cerium-iodide distance in e.g. $NaCe_4N_2I_7$ ($d_{min}(Ce^{3+}–I^-)$=313 pm) is slightly shorter than in $Ce_{15}N_7I_{24}$ (317 pm) [17], as a comparable compound. Otherwise, in the ethanide iodides $La_5(C_2)I_9$ (orthorhombic modification: 316 pm [28]; triclinic modification: 317 pm [29]) and $Nd_{12}(C_2)_3I_{17}$ (308 pm) [30] as well as in K_2PrI_5 (317 pm) [31] as ternary examples, the shortest metal-iodide distances are as small as in the $NaM_4N_2I_7$ series (M=La–Nd) (see Table 3). The longest regular metal-iodine bonds, which occur

around 383 pm with δ-ECoN values [23] for primary M^{3+}–I^{-} contacts larger than 0.176, and the distances for secondary interactions between 395 and 416 pm (δ-ECoN [23] for secondary M^{3+}–I^{-} contacts between 0.113 and 0.023; dotted lines in Fig. 1) are again in good agreement with those in rather similar compounds. For the binary triiodide LaI_3 (334–340 pm) [32] and in the oxide iodides *M*OI ($d(M^{3+}$–$I^{-})$=348 pm for *M*=La and 341 pm for *M*=Pr) [33,34] the distances are significantly longer, but they agree well with the average distances of the so-called regular M^{3+}–I^{-} bonds of the $NaM_4N_2I_7$ series ($d(M^{3+}$–$I^{-})$=343 pm for *M*=La, 341 pm for *M*=Ce, 339 pm for *M*=Pr and 337 pm for *M*=Nd).

Table 5
Classification of the infrared bands (in cm^{-1}) of the substances NaI, MI_3 and $NaM_4N_2I_7$ (*M*=La–Nd).

NaI	LaI_3	CeI_3	PrI_3	NdI_3	Ident.
	114[a]	114[a]	115[a]	115[a]	*M*–I
117					Na–I
	158	160	163	165	*M*–I
166					Na–I
$NaM_4N_2I_7$	*M*=La	*M*=Ce	*M*=Pr	*M*=Nd	
	117[a]	118[a]	117[a]	118[a]	Na–I/*M*–I
	167	166	168	164	Na–I
	337	338	352	364	*M*–N
	373	377	390	395	*M*–N
	489[a]	490[a]	499[a]	503[a]	*M*–N

[a] With shoulder.

The distances between metal cations and nitride anions (222–244 pm) in the title compounds differ not much from the observed distances in La_2NCl_3 (236 pm) [11], $Ce_{15}N_7I_{24}$ (217–239 pm) [17], Pr_2NCl_3 (233 pm) [10] or Nd_2NCl_3 (231–232 pm) [10], in which the same dominating structural features, $^{1}_{\infty}\{[NM^{e}_{4/2}]^{3+}\}$ chains built of *trans*-edge connected $[NM_4]^{9+}$ tetrahedra namely, are found likewise. In these chains, the $N^{3-}\cdots N^{3-}$ distances (288–311 pm) are in good agreement with those seen in $Ce_{15}N_7I_{24}$ (301–316 pm) [17] and Gd_2NBr_3 (293–298 pm) [12], but they are a little bit shorter than in the

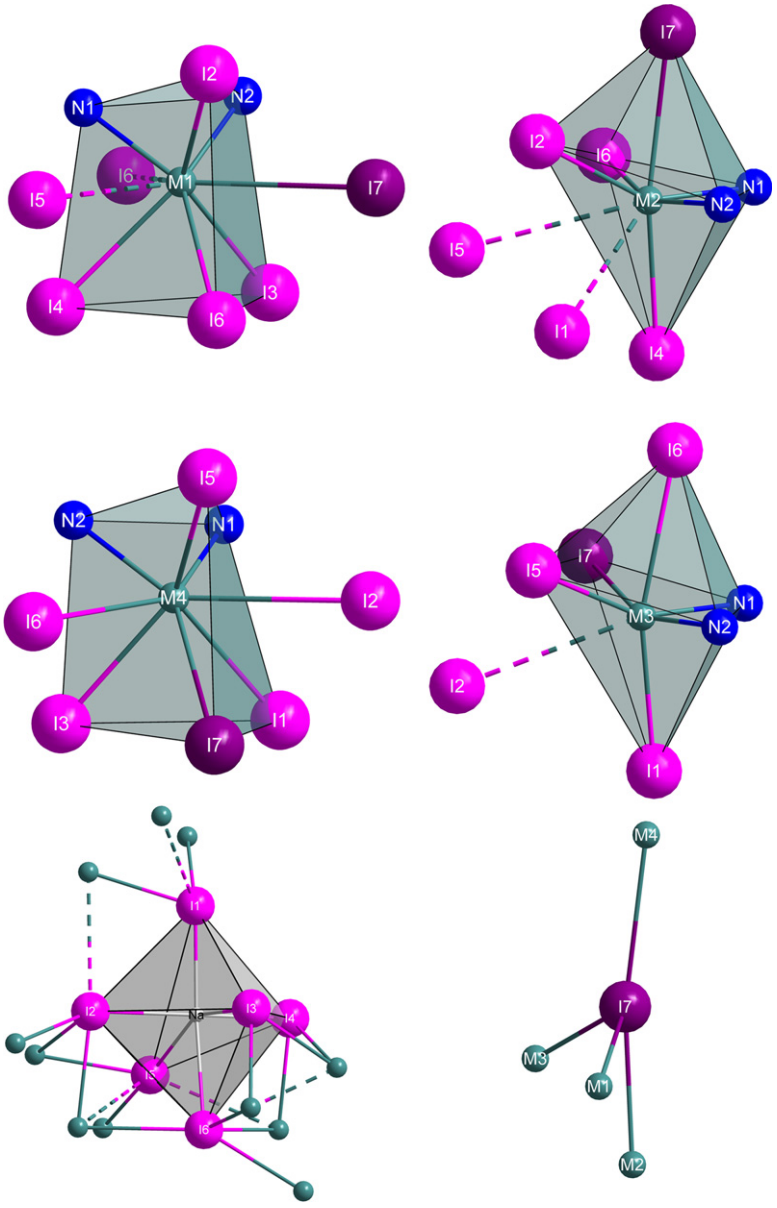

Fig. 1. Coordination spheres of the $(M1)^{3+}$ (*left top*), $(M2)^{3+}$ (*left mid*), $(M3)^{3+}$ (*right mid*), $(M4)^{3+}$ cations (*right top*), the isolated distorted $[NaI_6]^{5-}$ octahedron with all outer I^{-}–M^{3+} bonds (*left bottom*) and the special coordinative environment of $(I7)^{-}$ (*right bottom*) in the crystal structure of the nitride iodides $NaM_4N_2I_7$ (*M*=La–Nd).

$M_4N_2Te_3$ series (M=La–Nd; $d(N^{3-}\cdots N^{3-})$=303–311 pm for M=La, 300–307 pm for M=Ce, 298–305 pm for M=Pr and 297–303 pm for M=Nd) [35], which show the same trend from M=La to Nd as in the title compounds (see Table 3) caused by the lanthanide contraction. However, in the crystal structure of the $NaM_4N_2I_7$ series (M=La–Nd), these chains for the first time run parallel to a polar axis, namely [001] (Fig. 3). Two direct bonds (I6 and I7) and two secondary contacts (I2 and I5) to the M^{3+} cations link the chains to form a three-dimensional framework where several iodides from the $[NaI_6]^{5-}$ octahedra are bonded to the trivalent cations of the $^1_\infty\{[NM^e_{4/2}]^{3+}\}$ chains (Fig. 4). Hence, regarding those chains along with the only directly fourfold bonded $(I7)^-$ anions (Fig. 1, *right bottom*) a three-dimensional framework $^3_\infty\{[M_4N_2I]^{5+}\}$ results with cages, in which isolated distorted $[NaI_6]^{5-}$ octahedra (Fig. 1, *left bottom*) are embedded ($d(Na^+–I^-)$= 298–338 pm; Figs. 4 and 5). The bond lengths between sodium and iodide are reminiscent of those in e.g. $NaInI_4$ (294–365 pm) [36] and even the binary NaI (324 pm) [37,38]. A splitting of the formula $NaM_4N_2I_7$ (M=La–Nd) into $[NaI][M_2NI_3]_2$ reflects the dominating structural features of $^1_\infty\{[NM^e_{4/2}]^{3+}\}$ chains quite well, which can also be observed in the ternary lanthanide nitride halides M_2NX_3 (M=La–Gd, X=Cl, Br) [10–12], along with the $[NaI_6]^{5-}$ octahedra as building blocks cut out of rocksalt-type sodium iodide NaI [37,38]. A similar behavior of the main structural motifs is reported for $CsNaLa_6N_2Br_{14}$ (≡$[CsBr][NaBr][La_3NBr_6]_2$) [16], in which the bitetrahedral units

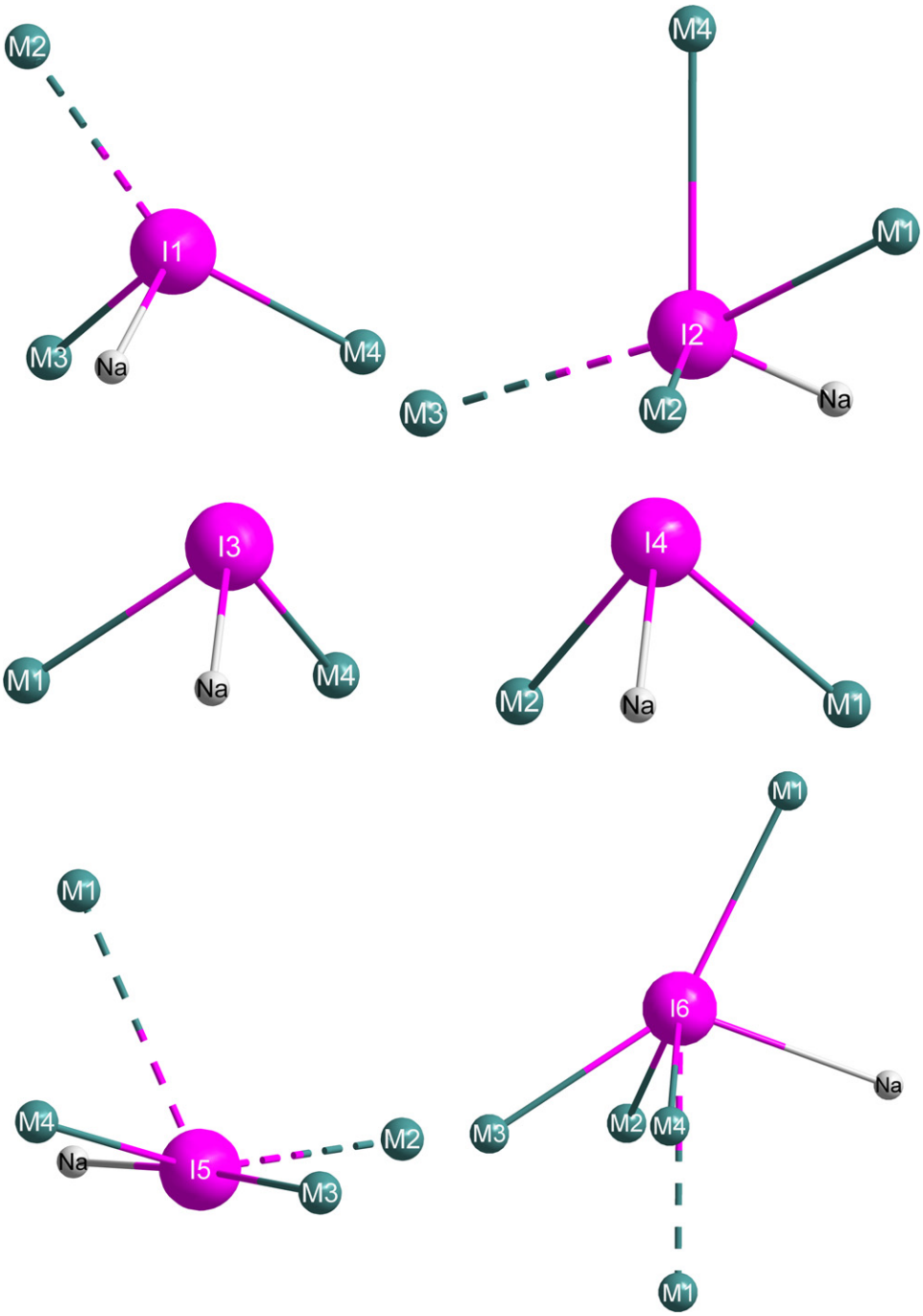

Fig. 2. Coordination spheres with all primary and secondary bonds of the $(I1)^-$ (*left top*), $(I2)^-$ (*right top*), $(I3)^-$ (*left mid*), $(I4)^-$ (*right mid*), $(I5)^-$ (*left bottom*) and $(I6)^-$ anions (*right bottom*) in the crystal structure of the nitride iodides $NaM_4N_2I_7$ (M=La–Nd).

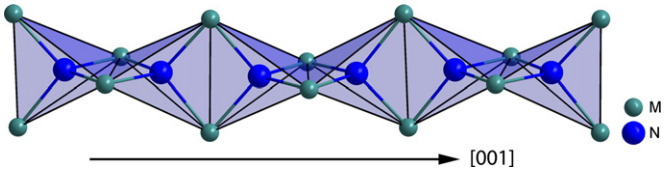

Fig. 3. The dominating structural features of $^{1}_{\infty}\{[NM^{e}_{4/2}]^{3+}\}$ chains built of *trans*-edge shared $[NM_4]^{9+}$ tetrahedra running along [001] in the crystal structure of the nitride iodides $NaM_4N_2I_7$ (M=La–Nd).

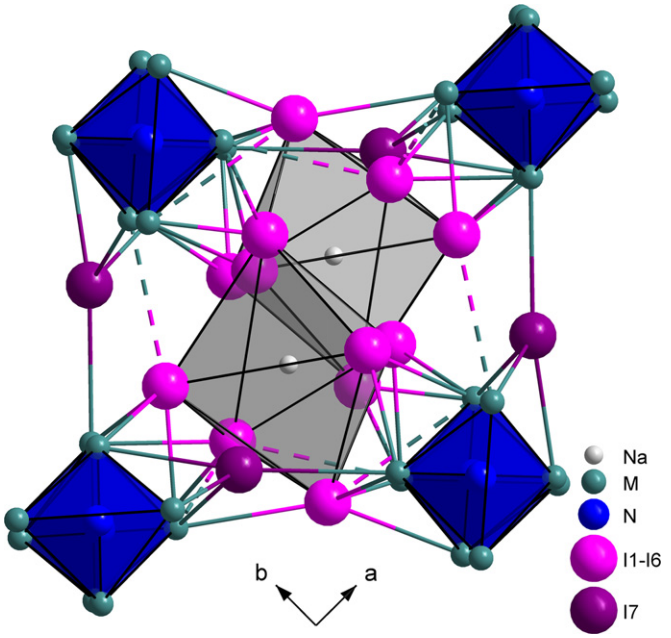

Fig. 4. View at the connections between the $^{1}_{\infty}\{[NM^{e}_{4/2}]^{3+}\}$ chains and the isolated distorted $[NaI_6]^{5-}$ octahedra in the crystal structure of the nitride iodides $NaM_4N_2I_7$ (M=La–Nd).

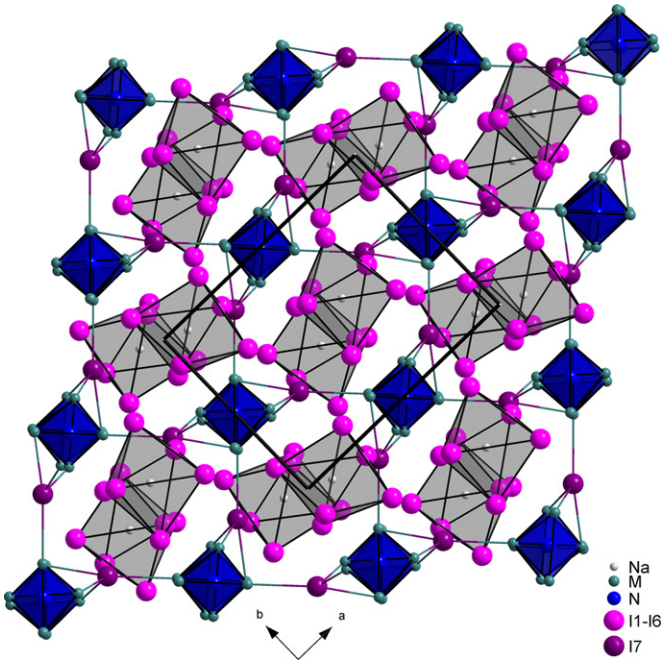

Fig. 5. View at the three-dimensional framework $^{3}_{\infty}\{[M_4N_2I]^{5+}\}$ with isolated $[NaI_6]^{5-}$ octahedra within the cages in the crystal structure of the nitride iodides $NaM_4N_2I_7$ (M=La–Nd).

$[M_6N_2]^{12+}$ as known from the M_3NBr_6-type nitride bromides (M=La, Ce) [12,16] are observed together with (edge sharing) $[NaBr_6]^{5-}$ octahedra recruiting building blocks from rocksalt-type sodium bromide NaBr [37,38]. Treating the only known ternary nitride iodide of the lanthanides $Ce_{15}N_7I_{24}$ [17] the same way, its formula can be split according to $[Ce_3NI_6]_4[Ce_2NI_3]_{24}$. The first part reflects the $^{1}_{\infty}\{[NCe^{e}_{2/2}Ce^{v}_{1/2}]^{1.5+}\}$ chains consisting of edge- and vertex-linked $[NCe_3]^{6+}$ triangles and the second one the $^{1}_{\infty}\{[NM^{e}_{4/2}]^{3+}\}$ chains of *trans*-edge shared $[NCe_4]^{9+}$ tetrahedra of the fictive compound Ce_2NI_3. Thus, it can be assumed that compounds of the composition M_2NI_3 should be synthesizable as well and that it is likely to obtain alkali-metal containing nitride chlorides and nitride bromides of the lanthanides too.

As to the secondary contacts between the lanthanide cations M^{3+} and the $(I2)^{-}$ and $(I5)^{-}$ anions, it should be mentioned, that in contradiction to the lanthanide contraction (for CN=8: $r(La^{3+})$=116.0 pm, $r(Ce^{3+})$=114.3 pm, $r(Pr^{3+})$=112.6 pm, $r(Nd^{3+})$=110.9 pm [26]) the distances between M^{3+} (M=La–Nd) and these iodide anions increase with decreasing radius of the lanthanide trication ($d(M3^{3+}–I2^{-})$=395 pm for M=La, 399 pm for M=Ce, 403 pm for M=Pr, 406 pm for M=Nd and $d(M2^{3+}–I5^{-})$=400 pm for M=La, 403 pm for M=Ce, 407 pm for M=Pr, 412 pm for M=Nd). This goes along with further observations. Firstly, the lanthanide contraction causes slightly shorter $M^{3+}–N^{3-}$ bonds (M=La: 233–239 pm to M=Nd: 224–237 pm) and secondly, the bond lengths between sodium and iodide are relatively short, but rigid. Thus, the $[NaI_6]^{5-}$ octahedra need the same amount of space within each of the quaternary nitride iodides $NaM_4N_2I_7$ from M=La to Nd. In correlation with this the direct bonds via $(I6)^{-}$ and $(I7)^{-}$ between the $^{1}_{\infty}\{[NM^{e}_{4/2}]^{3+}\}$ chains decrease only slightly following the lanthanide contraction. In each case two bonds (I6/I7–*M*2 and I6/I7–*M*3, see Table 3) become shorter, one become longer (I6–*M*4) and the other bonds (I6/I7–*M*1 and I7–*M*4, see Table 3) remain nearly unaffected. It can be assumed that the amount of space, which the unchanged $[NaI_6]^{5-}$ octahedra need, along with the demands of the lanthanide contraction, leads to such a structural realignment. Thus, we expect that the *non*-centrosymmetric structure of the $NaM_4N_2I_7$ representatives (M=La–Nd, Fig. 7) can no longer be maintained with the heavier lanthanides, as may also be seen in both structures of the M_2NCl_3 series with M=La–Pr in *Ibam*, but in *Pbcn* with M=Nd, Gd [9–11], for example, which also contain analogous $^{1}_{\infty}\{[NM^{e}_{4/2}]^{3+}\}$ chains.

3.2. Infrared measurements and interpretation

To compare the measured IR spectra of the $NaM_4N_2I_7$ title compounds with less complex situations, additional IR spectra of NaI and MI_3 (M=La–Nd) were collected separately. As expected, the infrared spectra of NaI and MI_3 (M=La–Nd; Fig. 6, *top*) show only bands below wavenumbers of about 200 cm^{-1}. The decrease of the transmission and the bands at υ=117 and 166 cm^{-1} in NaI are comparable to those observed in KI and RbI (υ=114/140 and 85/110 cm^{-1}) [39], all displaying the rocksalt-type crystal structure.

The infrared spectra of the whole $NaM_4N_2I_7$ series (M=La–Nd, see Table 5) between 100 and 400 cm^{-1} (Fig. 7, *top*) as well as between 400 and 1000 cm^{-1} (Fig. 7, *bottom*) show the same characteristics. Thus, in all spectra the bands at υ=117 and 166 cm^{-1} seem to be comparable with those of sodium iodide NaI. This is supported by the fact that in the quaternary nitride iodides as well as in NaI itself $[NaI_6]^{5-}$ octahedra are present as main structural features [20,37,38]. In the IR spectra of the triiodides MI_3 and the $NaM_4N_2I_7$-type quaternaries (M=La–Nd), shoulders

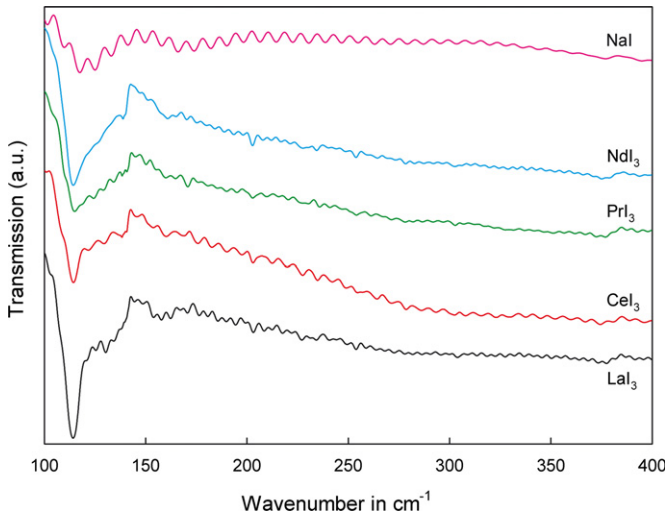

Fig. 6. Infrared spectra of NaI and MI_3 (M=La–Nd) from 100 to 400 cm^{-1}.

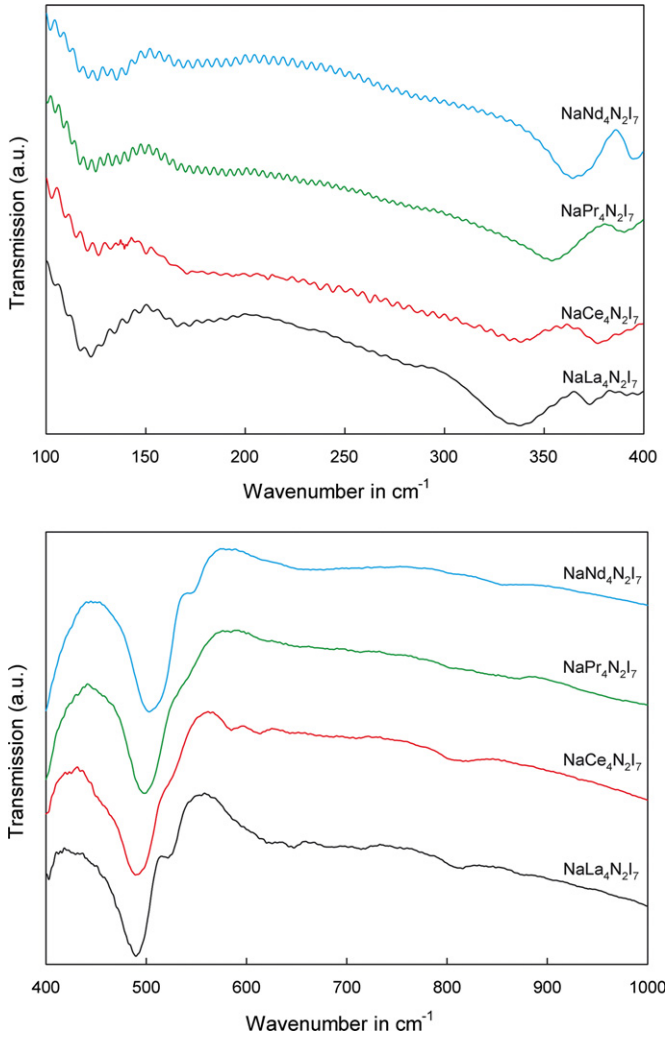

Fig. 7. Infrared spectra of the nitride iodides $NaM_4N_2I_7$ (M=La–Nd) between 100 and 400 cm^{-1} (*top*) as well as between 400 and 1000 cm^{-1} (*bottom*).

below wave numbers of υ=140 cm^{-1} are noticeable for all, which may be an evidence for M–I vibrations [20,40–48] in both kinds of compounds. Each of the three bands above a wavenumber of about 200 cm^{-1}, which could be measured in every $NaM_4N_2I_7$ representative, can probably be assigned to the vibrations of the $[NM_4]^{9+}$ tetrahedra as main structural features in the title compounds (Table 5). This finding is confirmed by the observation that in this range no bands are detected in the spectra of either NaI or the MI_3 representatives (M=La–Nd) [20,40–48]. Furthermore and well within our expectations, these three IR bands are shifted toward higher frequencies and thus energies with decreasing size of the involved M^{3+} cation (Table 5) [41], which is also observed for Raman spectra of other lanthanide compounds, such as the oxide selenides $M_4O_4Se[Se_2]$ (M=La–Nd, Sm) [49]. As already known for such hard ionic compounds as those of the $NaM_4N_2I_7$ series (M=La–Nd), no further bands were obtained above wavenumbers of 1000 cm^{-1} contrary to compounds containing highly covalent building blocks like $MClMoO_4$ (M=La–Pr) as examples with condensed $[MoO_{4+1}]^{4-}$ units [50]. Although a complete exclusion of pressure effects or an influence of KBr or PE in addition to the pressure is not possible, we strongly assume that there are no such issues present, since the colors of the pellets were the same as for the selected crystals (even after their measurements) and an unusual shift or splitting of the bands could not be observed.

By comparing the infrared spectrum of $NaLa_4N_2I_7$ with literature data, a more detailed discussion about the band positions is difficult, because no investigations of La^{3+}- and N^{3-}-bearing compounds (with $CN(N^{3-})=4$) are available so far, except for the binary rocksalt-type nitride LaN ($CN(N^{3-})=6$) itself with bands centered at about 650 cm^{-1} [51,52]. This also holds for compounds like Eu_2OI_2 [53], $Na_2M_4ONCl_9$ (M=Ce, Nd, Gd) [11,54,55] and $A_2Pr_4O_2Cl_2$ (A=Na, K) [56], in which structurally similar acting oxide anions reside partly or completely at the sites of nitride anions in the infinite chains of *trans*-edge shared cation tetrahedra. Thus, we compare our results with the O^{2-}-containing sulfide $GaLa_3OS_5$ with infinite $^1_\infty\{[OLa^e_{3/3}La^t_{1/1}]^{4+}\}$ chains of *cis*-edge linked $[OLa_4]^{10+}$ tetrahedra according to $[La_2O]GaLaS_5$ [57,58]. *Barnier et al.* [59] assigned the La–O vibrations in $GaLa_3OS_5$ to Raman bands at around υ=377 and 395 cm^{-1} and in the binary A-type La_2O_3 ($=^2_\infty\{[La_2O_2]\}O$) [59] to bands from υ=364 to 395 cm^{-1}. In the IR spectrum of $NaLa_4N_2I_7$ strong bands occur in this range (υ=337 and 373 cm^{-1}) as well, although they are shifted to slightly smaller wavenumbers here. This shift can be well explained by considering the different light elements involved (*Barnier et al.*: oxygen, *here*: nitrogen). The third and small fourth band (υ=489 and 520 cm^{-1}) may indicate a difference in the connectivity features of the entire tetrahedra (*Barnier et al.*: $^1_\infty\{[OLa^e_{3/3}La^t_{1/1}]^{4+}\}$ chains of *cis*-edge shared $[OLa_4]^{10+}$ tetrahedra, *here*: $^1_\infty\{[NLa^e_{4/2}]^{3+}\}$ chains of *trans*-edge shared $[NLa_4]^{9+}$ tetrahedra). Thus, we strongly assume that these $^1_\infty\{[NM^e_{4/2}]^{3+}\}$ chains with their edge-linked $[NLa_4]^{9+}$ entities are finally responsible for the IR bands at υ=337, 373 and 489 cm^{-1}. For the near future, IR and Raman investigations with the isotypic triple $La_4NS_3Cl_3$ [19], $La_4NSe_3Cl_3$ [60] and $La_4NS_3Br_3$ [60] with completely isolated $[NLa_4]^{9+}$ tetrahedra are planned for comparison.

4. Conclusion

In this paper the crystal structure of the first quaternary lanthanide(III) nitride iodides with the composition $NaM_4N_2I_7$ (M=La–Nd) is described as well as their syntheses and some spectroscopic properties. The crystal structure recruits two main features, namely $^1_\infty\{[NM^e_{4/2}]^{3+}\}$ chains consisting of *trans*-edge sharing $[NM_4]^{9+}$ tetrahedra and isolated distorted $[NaI_6]^{5-}$ octahedra. Thereby the latter are embedded within a three-dimensional framework $^3_\infty\{[M_4N_2I]^{5+}\}$ erected by the interconnection of the $^1_\infty\{[NM^e_{4/2}]^{3+}\}$ chains via a special iodide

anions. In the IR spectra, ranges for the typical M^{3+}–N^{3-} vibrations within these $^{1}_{\infty}\{[NM^{e}_{4/2}]^{3+}\}$ chains were determined for the first time ever.

Acknowledgments

We thank *Dr. Sabine Strobel* and *Dr. Ingo Hartenbach* for the measurement of the X-ray single-crystal diffraction data sets as well as *Dipl.-Chem. Karin Aniol* for her practical work. Our thank also goes to *Dipl.-Chem. Fanny Schurz* (Research Group of *Prof. Dr. Dr. h. c. Martin Jansen*) and *Wolfgang König* (Spectroscopy Service Group), both at the Max-Planck Institute for Solid-State Research, Stuttgart, for their IR measurements. Furthermore, we gratefully acknowledge the considerable financial support of the "Land Baden-Württemberg" (Stuttgart) and the "Fonds der Chemischen Industrie" (Frankfurt a. M.).

References

[1] D. Bright, J.A. Ibers, Inorg. Chem. 8 (1969) 709–716.
[2] Ch. Wachsmann, H. Jacobs, Z. Anorg. Allg. Chem. 622 (1996) 885–888.
[3] D.A. Headspith, M.G. Francesconi, Top. Catal. 52 (2009) 1611–1627.
[4] M.G. Francesconi, M.G. Barker, C. Wilson, Chem. Commun. (2002) 1358–1359.
[5] A.D.J. Barnes, T.J. Prior, M.G. Francesconi, Chem. Commun. (2007) 4638–4640.
[6] X. Chen, L. Zhu, S. Yamanaka, J. Solid State Chem. 169 (2002) 149–154.
[7] J. Oró-Solé, C. Frontera, D. Beltrán-Porter, O.I. Lebedev, G. van Tendeloo, A. Fuertes, Mater. Res. Bull. 41 (2006) 934–940.
[8] J. Oró-Solé, C. Frontera, B. Martínez, D. Beltrán-Porter, M.R. Palacín, A. Fuertes, Chem. Commun. (2005) 3352–3354.
[9] U. Schwanitz-Schüller, A. Simon, Z. Naturforsch. 40b (1985) 705–709.
[10] S. Uhrlandt, G. Meyer, J. Alloys Compds. 225 (1995) 171–173.
[11] C.M. Schurz, Th. Schleid, J. Alloys Compds. 485 (2009) 110–118.
[12] Hj. Mattausch, A. Simon, Z. Kristallogr. NCS 211 (1996) a) 397, b) 398, c) 399.
[13] A. Simon, T. Köhler, J. Less-Common Met. 116 (1986) 279–292.
[14] (a) G.M. Ehrlich, M.E. Badding, N.E. Brese, S.S. Trail, F.J. DiSalvo, J. Alloys Compds. 206 (1994) 95–101;
(b) G.M. Ehrlich, M.E. Badding, N.E. Brese, S.S. Trail, F.J. DiSalvo, J. Alloys Compds. 235 (1996) 133–134.
[15] M. Meyer, F. Lissner, Th. Schleid, Z. Anorg. Allg. Chem. 626 (2000) 1205–1210.
[16] M. Lulei, Inorg. Chem. 37 (1998) 777–781.
[17] Hj. Mattausch, R.K. Kremer, A. Simon, Z. Anorg. Allg. Chem. 622 (1996) 649–654.
[18] M. Lulei, J.D. Corbett, Eur. J. Solid State Inorg. Chem. 33 (1996) 241–250.
[19] (a) F. Lissner, Th. Schleid, Z. Anorg. Allg. Chem. 620 (1994) 1998–2002;
(b) Th. Schleid, M. Meyer, Z. Kristallogr. 211 (1996) 187;
(c) C.M. Schurz, F. Lissner, Th. Schleid, Z. Kristallogr. (Suppl. 29) (2009) 38.
[20] C.M. Schurz, K. Aniol, Th. Schleid, Z. Anorg. Allg. Chem. 634 (2008) 2079.
[21] G.M. Sheldrick, SHELX-97: Program Package for Crystal Structure Solution and Refinement, Göttingen (1997).
[22] (a) A.L. Spek, in: PLATON: A Multipurpose Crystallographic Tool, Utrecht University, Utrecht, The Netherlands, 2008;
(b) A.L. Spek, J. Appl. Crystallogr. 36 (2003) 7–13.
[23] (a) R. Hoppe, Izvj. Jugoslav. Centr. Krist. 8 (1973) 21;
(b) R. Hoppe, Angew. Chem. 78 (1966) 52;
(c) R. Hoppe, Angew. Chem. 82 (1970) 7;
(d) R. Hoppe, Angew. Chem. 92 (1980) 106;
(e) R. Hoppe, Angew. Chem., Int. Ed. 5 (1966) 95;
(f) R. Hoppe, Angew. Chem., Int. Ed. 9 (1970) 25;
(g) R. Hoppe, Angew. Chem., Int. Ed. 19 (1980) 110;
(h) C.J.M. Rooymans, A. Rabenau (Eds.), Crystal Structure and Chemical Bonding in Inorganic Chemistry, Amsterdam (1975).
[24] W. Herrendorf, H. Bärnighausen, in: HABITUS: A Program for the Optimization of the Crystal Shape for Numerical Absorption Correction in X-SHAPE, Version 1.06, Fa. Stoe, Darmstadt, Karlsruhe, Germany, 1996.
[25] Th. Hahn, A.J.C. Wilson (Eds.), International Tables for Crystallography, vol. C, 2nd ed., Kluwer Academic Publishers, Boston, MA, 1992.
[26] R.D. Shannon, Acta Crystallogr. A 32 (1976) 751–767.
[27] R.X. Fischer, E. Tillmanns, Acta Crystallogr. C 44 (1988) 775–776.
[28] Hj. Mattausch, C. Hoch, A. Simon, Z. Anorg. Allg. Chem. 634 (2008) 641–645.
[29] Hj. Mattausch, C. Hoch, A. Simon, Z. Anorg. Allg. Chem. 631 (2005) 1423–1429.
[30] M. Ryazanov, Hj. Mattausch, A. Simon, J. Solid State Chem. 180 (2007) 1372–1380.
[31] G. Meyer, J. Soose, A. Moritz, V. Vitt, Th. Holljes, Z. Anorg. Allg. Chem. 521 (1985) 161–172.
[32] W.H. Zachariasen, Acta Crystallogr. 1 (1948) 265–268.
[33] L.G. Stiller, A.L. Nylander, Svensk Kem. Tidskr. 53 (1941) 367–372.
[34] O.G. Potapova, I.G. Vasil'eva, S.V. Borisov, Zh. Strukt. Khim. 18 (1977) 573–577.
[35] F. Lissner, Th. Schleid, Z. Anorg. Allg. Chem. 631 (2005) 1119–1124.
[36] Th. Staffel, G. Meyer, Z. Anorg. Allg. Chem. 574 (1989) 107–113.
[37] H.E. Swanson, W.P. Davey, Phys. Rev. 21 (1923) 143–161.
[38] E. Posnjak, R.W.G. Wyckoff, J. Washington Acad. Sci. 12 (1922) 248–251.
[39] R.A. Nyquist, R.O. Kagel, in: Handbook of Infrared and Raman Spectra of Inorganic Compounds and Organic Salts; Vol. 4: Infrared Spectra of Inorganic Compounds (3800–45 cm^{-1}), Academic Press, Inc., San Diego, CA, 1997.
[40] J.C. Wells Jr., J.B. Gruber, M. Lewis, Chem. Phys. 24 (1977) 391–397.
[41] A. Kovács, R.J.M. Konings, J. Phys. Chem. Ref. Data 33 (2004) 377–404.
[42] A. Kovács, R.J.M. Konings, Chem. Phys. Lett. 268 (1997) 207–212.
[43] C. Adamo, P. Maldivi, J. Phys. Chem. A 102 (1998) 6812–6820.
[44] V.G. Solomonik, O.Y. Marochko, Russ. J. Phys. Chem. 74 (2000) 2094–2096.
[45] A. Kovács, J. Mol. Struct. 482–483 (1999) 403–407.
[46] T. Nilges, Z. Naturforsch. 61b (2006) 117–122.
[47] A. Kovács, Chem. Phys. Lett. 319 (2000) 238–246.
[48] G. Oczko, L. Macalik, J. Legendziewicz, J. Hanuza, J. Alloys Compds. 380 (2004) 327–336.
[49] S. Strobel, A. Choudhury, P.K. Dorhout, C. Lipp, Th. Schleid, Inorg. Chem. 47 (2008) 4936–4944.
[50] I. Hartenbach, Th. Schleid, S. Strobel, P.K. Dorhout, Z. Anorg. Allg. Chem. 636 (2010) 1183–1189.
[51] K. Nakamoto, in: Infrared and Raman of Inorganic and Coordination Compounds, 3rd ed., Wiley, New York, 1978.
[52] I.P. Parkin, A.M. Nartowski, Polyhedron 17 (1998) 2617–2622.
[53] S. Hammerich, G. Meyer, Z. Anorg. Allg. Chem. 632 (2006) 1244–1246.
[54] C.M. Schurz, M. Meyer, G. Meyer, Th. Schleid, Z. Anorg. Allg. Chem. 636 (2010) 1169–1171.
[55] U. Beck, A. Simon, Z. Anorg. Allg. Chem. 623 (1997) 1011–1016.
[56] H. Mattfeld, G. Meyer, Z. Anorg. Allg. Chem. 620 (1994) 85–89.
[57] S. Jaulmes, A. Mazurier, M. Guittard, Acta Crystallogr. C 39 (1983) 1594–1597.
[58] M. Guittard, S. Jaulmes, A.M. Loireau-Lozach, A. Mazurier, F. Berguer, J. Flahaut, J. Solid State Chem. 58 (1985) 276–289.
[59] S. Barnier, C. Julien, M. Guittard, Spectrochim. Acta 44A (1988) 709–712.
[60] M. Meyer, Dissertation, Universität Hannover (1996).